

~~CONFIDENTIAL~~

CB No. L6B26

NATIONAL ADVISORY COMMITTEE FOR AERONAUTICS

Declassified

WARTIME REPORT

ORIGINALLY ISSUED

April 1946 as

~~Confidential~~ Bulletin L6B26

INTERNAL AND EXTERNAL AERODYNAMICS OF DUCTED
BODIES AT SUPERSONIC SPEEDS

By Clinton E. Brown

Langley Memorial Aeronautical Laboratory
Langley Field, Va.

NACA

WASHINGTON

NACA WARTIME REPORTS are reprints of papers originally issued to provide rapid distribution of advance research results to an authorized group requiring them for the war effort. They were previously held under a security status but are now unclassified. Some of these reports were not technically edited. All have been reproduced without change in order to expedite general distribution.

NATIONAL ADVISORY COMMITTEE FOR AERONAUTICS

CONFIDENTIAL BULLETIN

INTERNAL AND EXTERNAL AERODYNAMICS OF DUCTED
BODIES AT SUPERSONIC SPEEDS

By Clinton E. Brown

SUMMARY

A method for calculating the lift, moment, and pressure drag of slender open-nose bodies of revolution at supersonic speeds is described. An application of the method to a typical ram-jet fuselage is shown to give excellent agreement with available experimental data. A drag comparison was omitted because of the presence of skin-friction drag in the experimental drag data. The problem of obtaining high total-pressure recovery at supersonic speeds is discussed and some experimental data obtained at the Langley Memorial Aeronautical Laboratory of the NACA on circular diffusers is presented. It is pointed out that variable-geometry diffusers might be designed to give high diffuser efficiencies over a wide range of Mach number.

INTRODUCTION

Work on ram-jet housing bodies was started at the NACA in the summer of 1943. At that time, no experimental data of any kind were available in this country on ducted bodies at supersonic speeds. As work progressed, an open-nose body of revolution was selected as a fuselage for a possible supersonic airplane. A test program was started in the Langley model supersonic tunnel and a 5-inch model of the fuselage selected was tested at several Mach numbers. Curves from these data were obtained of lift, moment, and drag coefficients. In conjunction with the test program, an investigation was begun to find means for calculating the aerodynamic characteristics of these bodies. As a result, a method was found (reference 1) which, for the body tested, gave excellent agreement with the experimental results. Previous to this work, a series of tests were conducted

in a 1-inch supersonic jet at the Langley Memorial Aeronautical Laboratory on circular diffusers having a small contraction just behind the duct entrance (reference 2). Some of the results obtained are presented and discussed.

The discussion given in the present paper was originally presented at a Symposium on Supersonic Flow held at the Johns Hopkins University, Applied Physics Laboratory, Silver Spring, Md., on Dec. 6 and 7, 1945.

SYMBOLS

x, r, θ cylindrical coordinates

X distance along X -axis measured from nose of body

l length of body

R radius of body

β Mach angle $(\sin^{-1} \frac{1}{M})$

$$B = \sqrt{M^2 - 1}$$

$\phi(x, r, \theta)$ perturbation potential

$\phi_1(x, r)$ perturbation potential for axial flow

$\phi_2(x, r, \theta)$ perturbation potential for cross flow

v_x axial velocity increment $(\frac{\partial \phi}{\partial x})$

v_r radial velocity increment $(\frac{\partial \phi}{\partial r})$

V velocity in undisturbed stream

- a velocity of sound in undisturbed stream
- M Mach number in undisturbed stream (V/a)
- ρ density in undisturbed stream
- Δp incremental surface pressure due to angle of attack
- p_l local pressure
- p pressure in undisturbed stream
- γ ratio of specific heats of air (1.4)
- α angle of attack, radians (except where otherwise noted)
- δ angle between surface of body and X-axis
- C_L lift coefficient $\left(\frac{\text{Lift}}{\frac{\rho V^2 \pi R_N^2}{2}} \right)$
- C_D drag coefficient $\left(\frac{\text{Drag}}{\frac{\rho V^2 \pi R_N^2}{2}} \right)$
- C_m moment coefficient $\left(\frac{\text{Moment}}{\frac{\rho V^2 \pi R_N^2 l}{2}} \right)$
- u variable of integration
- $\xi = x - Br \cosh u$
- $j_1 = x_1 - BR_1$
- $T_1^n = \frac{x_n - j_1}{BR_n}$
- $A_1 = f'(\xi)_1$

Subscripts and superscripts:

N refers to nose

n refers to n^{th} integration station, summation variablei refers to i^{th} integration station, summation variable

max maximum

deg in degrees

MATHEMATICAL ANALYSIS

Pointed Bodies of Revolution

The analysis that is presented herein is essentially that found in reference 1. The mathematical methods used were first developed by von Kármán and Moore (reference 3) and applied to the cone problem and to sharp-nose projectiles. If the problem is restricted to slender bodies, the differential equation of motion for a compressible fluid can be linearized to give, in cylindrical coordinates, the simple form

$$\frac{\partial^2 \phi}{\partial r^2} + \frac{1}{r} \frac{\partial \phi}{\partial r} + \frac{1}{r^2} \frac{\partial^2 \phi}{\partial \theta^2} = (M^2 - 1) \frac{\partial^2 \phi}{\partial x^2} \quad (1)$$

where ϕ is the potential function assumed to represent the effect of a small disturbance set up by the slender bodies being considered. The problem is, therefore, to find a solution of equation (1) that will satisfy the known boundary conditions at the surface of the body. A general solution of the differential equation (1) when $M > 1$, for diverging waves has been found by Lamb (reference 4) to be, with a slight change in notation:

$$\phi = \sum_s Q_s r^s \cos s\theta + P_s r^s \sin s\theta$$

where

$$Q_s = \left(\frac{\partial}{r \partial r} \right)^s Q_0 \quad \left. \begin{array}{l} \\ \end{array} \right\} \quad (2)$$

$$P_s = \left(\frac{\partial}{r \partial r} \right)^s P_0 \quad \left. \begin{array}{l} \\ \end{array} \right\}$$

and

$$Q_0 = \int_0^\infty f(x - Br \cosh u) du$$

$$P_0 = \int_0^\infty g(x - Br \cosh u) du$$

where

$$B = \sqrt{x^2 - 1}$$

The part of Lamb's general solution corresponding to converging waves does not apply to the present problem since all disturbances originate on the body and diverge into the flow field investigated. Von Kármán and Moore have investigated the problem of the resistance of projectiles and cones (reference 3) and have found a solution for the case of axial symmetry

$$\phi = - \int_0^\infty f(x - Br \cosh u) du \quad (3)$$

which can be seen to be a special case of the general solution with $s = 0$. In their analysis it was found that the body, in this case a sharp-nose projectile, could be

represented by a distribution of sources along the X-axis starting at $x \equiv 0$, the nose of the body. By a numerical method of integration the equations for the velocity increments v_r and v_x could then be written

$$v_{r_n} = -B \sum_{i=1}^n A_i \left[\sqrt{(T_i^n)^2 - 1} - \sqrt{(T_{i-1}^n)^2 - 1} \right] \quad (4)$$

$$v_{x_n} = \sum_{i=1}^n A_i \left[\cosh^{-1}(T_i^n) - \cosh^{-1}(T_{i-1}^n) \right] \quad (5)$$

where

$$T_i^n = \frac{x_n - j_i}{BR_n}$$

and

$$j_i = x_i - BR_i$$

$$A_i = f'(\xi)_i$$

with the boundary conditions

$$\frac{v_r}{v + v_x} = \frac{dr}{dx} \quad (6)$$

These three equations in three unknowns (A_n, v_{r_n}, v_{x_n}) were solved at each station on the body for v_r and v_x .

The pressures were then found from the Bernoulli equation in the form:

$$\frac{p_l}{p} = \left[1 + \frac{\gamma - 1}{2} \left(-2M \frac{v_x}{a} - \frac{v_x^2 + v_r^2}{a^2} \right) \right]^{\frac{\gamma}{\gamma-1}} \quad (7)$$

Ferrari (reference 5) and Tsien (reference 6) have independently found solutions for the case of pointed bodies of revolution at small angles of attack. It was shown that the potential could be expressed in two terms: the first, from equation (3),

$$\phi_1 = - \int_0^\infty f_1(x - Br \cosh u) du$$

is the solution for the pure axial flow already described, and the second

$$\phi_2 = -B \cos \theta \int_0^\infty f_2(x - Br \cosh u) \cosh u du \quad (8)$$

represents the cross-flow potential of an arbitrary distribution of doublets along the axis of the body starting at the nose of the cone or projectile. The form of equation (8) is such that the cross flow is from the direction $\theta = 0$.

By neglecting the small effect of the axial flow on the lifting pressures, Tsien obtained for the pointed projectile of arbitrary shape the equations:

$$C_L = \frac{2a}{B} \sum_n \frac{x_{n+1} - x_n}{R_{base}} \frac{R_{n+1} + R_n}{R_{base}} \sum_{i=0}^n \frac{B^2 K_i}{2aV} \left[\sqrt{\left(\frac{T_{i-1}^n}{T_i^n}\right)^2 - 1} - \sqrt{\left(\frac{T_i^n}{T_{i-1}^n}\right)^2 - 1} \right] \quad (9)$$

$$C_m = -\frac{2a}{Bl} \sum_n \left[\frac{x_{n+1} + 2x_n}{3} + \left(\frac{x_{n+1} - x_n}{3} \frac{R_{n+1}}{R_{n+1} + R_n} \right) \right]$$

$$\left(\frac{x_{n+1} - x_n}{R_{Base}} \frac{R_{n+1} + R_n}{R_{Base}} \right) \sum_{i=0}^n \frac{B^2 K_i}{2aV} \left[\sqrt{\left(\frac{T_{i-1}^n}{T_i^n}\right)^2 - 1} - \sqrt{\left(\frac{T_i^n}{T_{i-1}^n}\right)^2 - 1} \right] \quad (10)$$

$$1 = \sum_{i=1}^n \frac{B^2 K_i}{2aV} \left[\cosh^{-1} \left(\frac{T_{i-1}^n}{T_i^n} \right) - \cosh^{-1} \left(\frac{T_i^n}{T_{i-1}^n} \right) \right]$$

$$+ \left(\frac{T_{i-1}^n}{T_i^n} \right) \sqrt{\left(\frac{T_{i-1}^n}{T_i^n}\right)^2 - 1} - T_i^n \sqrt{\left(\frac{T_i^n}{T_{i-1}^n}\right)^2 - 1} \quad (11)$$

The values K_i in these equations are assumed to be constants for each interval of the step-by-step process. The moment coefficient of equation (10) is assumed positive for nosing-up moments, the moments being taken about the nose.

Open-Nose Bodies

The flow conditions over an open-nose body differ from those of pointed bodies in that, for finite angles of the nose lip, the flow is two-dimensional at the lip. This problem was not considered in references 3, 5, and 6, and the general solution should therefore be examined to determine its applicability to this special case. It has been shown by Lamb (reference 4) that a sufficient requirement for the existence of the general solution to the differential equation of motion is that $f(x - Br \cosh u)$ be zero for all values of the argument less than some arbitrary limiting value. The determination of $f(x - Br \cosh u)$ such that the boundary conditions at the open-nose body are satisfied assures the fulfillment of this general requirement. For the usual case of supersonic flow into the nose, the boundary condition requires the surface of the body to be a continuation of a cylindrical stream surface of radius R_N in the undisturbed flow ahead of the body, as shown in figure 1. The perturbation potentials (equations (3) and (8)) must therefore be zero at the cylindrical stream surface ahead of the body. Substituting $\xi = x - Br \cosh u$ in equations (3) and (8) gives

$$\phi_1 = - \int_{-\infty}^{x-Br} \frac{f_1(\xi) d\xi}{\sqrt{(x - \xi)^2 - B^2 r^2}} \quad (12)$$

and

$$\phi_2 = - \frac{\cos \theta}{r} \int_{-\infty}^{x-Br} \frac{f_2(\xi)(x - \xi) d\xi}{\sqrt{(x - \xi)^2 - B^2 r^2}} \quad (13)$$

The boundary conditions are obviously satisfied when $f_1(\xi) = f_2(\xi) = 0$ for all values of $\xi < x_0 - Br_0$, where the point (x_0, R_0) is at the lip of the open-nose body. Values of $f_1(\xi)$ and $f_2(\xi)$ for $\xi > x_0 - Br_0$

then remain to be determined so that the body surface is a continuation of this stream surface. From physical considerations, $f_1(\xi)$ and $f_2(\xi)$ may be regarded as an axial distribution of sources and doublets, respectively, where ξ is measured along the X-axis. As the effect of a source or doublet can only be felt along or behind its Mach cone, the source distribution must begin a distance BR_0 ahead of the nose. This point is chosen for the origin of the coordinate system. It must be emphasized that the source and doublet distribution determined by satisfying the boundary conditions at the stream and body surfaces shown in figure 1 does not represent correctly the flow inside that stream surface. This result corresponds to the physical fact that the actual supersonic flow into the nose does not affect the flow external to the body. The basic assumptions of potential flow and small disturbances are valid provided the slope of the body surface is small. Actually, for finite angles of the nose lip, a nonconical shock wave is formed which causes a loss in total head and produces rotation in the field.

Numerical integration of equation (12), with constant values of $f_1'(\xi)$ over the integration intervals assumed, results in the same expressions for v_{r_n} and v_{x_n} as those obtained by von Kármán and Moore (equations (4) and (5)). These constant values of $f_1'(\xi)$ are determined by satisfying the boundary condition:

$$\frac{v_r}{v + v_x} = \tan \delta_n \quad (14)$$

where $\tan \delta_n$ is the slope of surface of the body at the n^{th} interval of integration.

By following the method of reference 5, the lift and moment coefficients for small angles of attack based on the area of the nose may be written

$$C_L = -\frac{4}{\pi R_N^2 V} \int_0^\pi \int_{BR_N}^{l+BR_N} \frac{\partial \phi_2}{\partial x} \cos \theta d\theta R dx \quad (15)$$

$$C_m = \frac{4}{\pi R_N^2 l V} \int_0^\pi \int_{BR_N}^{l+BR_N} \left(x - \frac{l}{2} - BR_N \right) \frac{\partial \phi_2}{\partial x} \cos \theta d\theta R dx \quad (16)$$

where l is the length of the body, R_N is the nose radius, and the moments are taken about the midpoint of the body. Substituting the expression for $\partial \phi_2 / \partial x$ in equations (15) and (16) gives, for C_L and C_m ,

$$C_L = \frac{4B}{\pi R_N^2 V} \int_0^\pi \cos^2 \theta d\theta \int_{BR_N}^{l+BR_N} R dx$$

$$\int_0^{x-BR} \frac{f_2'(\xi)(x-\xi)d\xi}{BR \sqrt{(x-\xi)^2 - B^2 R^2}} \quad (17)$$

$$C_m = -\frac{4}{\pi R_N^2 V l} \int_0^\pi \cos^2 \theta d\theta \int_{BR_N}^{l+BR_N} \left(x - \frac{l}{2} - BR \right) R dx$$

$$\int_0^{x-BR} \frac{f_2'(\xi)(x-\xi)d\xi}{BR \sqrt{(x-\xi)^2 - B^2 R^2}} \quad (18)$$

The distribution function $f_2(\xi)$ must be determined by the boundary condition

$$v_a \cos \theta = \left(\frac{\partial \phi_2}{\partial r} \right)_{r=R} \quad (19)$$

which assumes that the radial velocity is normal to the surface. A more rigorous boundary condition taking into account the slope of the body was given by Ferrari (reference 5). For small surface angles, however, equation (19) is within the accuracy of the small-perturbation assumptions. The expression

$$\left(\frac{\partial \phi_2}{\partial r} \right)_{r=R} = \frac{\cos \theta}{R^2} \int_0^{x-BR} \frac{f_2'(\xi)(x-\xi)^2 d\xi}{\sqrt{(x-\xi)^2 - B^2 R^2}} \quad (20)$$

is integrated numerically for constant values of $f_2'(\xi) = K_i$ over the i^{th} interval of integration to obtain the sum

$$\begin{aligned} \left(\frac{\partial \phi_2}{\partial r} \right)_{r=R} &= \frac{B^2 \cos \theta}{2} \sum_{i=1}^n k_i \left[\cosh^{-1}(T_{i-1}^{-n}) - \cosh^{-1}(T_i^{-n}) \right. \\ &\quad \left. + (T_{i-1}^{-n}) \sqrt{(T_{i-1}^{-n})^2 - 1} - T_i^{-n} \sqrt{(T_i^{-n})^2 - 1} \right] \end{aligned} \quad (21)$$

Substituting this equation in equation (19) gives

$$\begin{aligned} 1 &= \sum_{i=1}^n \frac{B^2 k_i}{2 v_a} \left[\cosh^{-1}(T_{i-1}^{-n}) - \cosh^{-1}(T_i^{-n}) \right. \\ &\quad \left. + (T_{i-1}^{-n}) \sqrt{(T_{i-1}^{-n})^2 - 1} - T_i^{-n} \sqrt{(T_i^{-n})^2 - 1} \right] \end{aligned} \quad (22)$$

With the values of $\frac{B^2 K_i}{2\alpha V}$ determined, equations (17) and (18) become

$$C_L = \frac{2\alpha}{R_N^2 B} \sum_n (x_n - x_{n-1})(R_n + R_{n-1}) \frac{1}{2} \left\{ \sum_{i=1}^n \frac{B^2 K_i}{2\alpha V} \left[\sqrt{(T_{i-1}^{-n})^2 - 1} - \sqrt{(T_i^{-n})^2 - 1} \right] \right. \\ \left. + \sum_{i=1}^{n-1} \frac{B^2 K_i}{2\alpha V} \left[\sqrt{(T_{i-1}^{-n-1})^2 - 1} - \sqrt{(T_i^{-n-1})^2 - 1} \right] \right\} \quad (23)$$

$$C_M = \frac{2\alpha}{R_N^2 B l} \sum_n \left(\frac{l + 2BR_N}{2} \right. \\ \left. - \frac{x_n + x_{n-1}}{2} \right) (x_n - x_{n-1})(R_n + R_{n-1}) \left(\frac{1}{2} \right) \left\{ \sum_{i=1}^n \frac{B^2 K_i}{2\alpha V} \left[\sqrt{(T_{i-1}^{-n})^2 - 1} - \sqrt{(T_i^{-n})^2 - 1} \right] \right. \\ \left. + \sum_{i=1}^{n-1} \frac{B^2 K_i}{2\alpha V} \left[\sqrt{(T_{i-1}^{-n-1})^2 - 1} - \sqrt{(T_i^{-n-1})^2 - 1} \right] \right\} \quad (24)$$

In equations (23) and (24) the pressure used for a given integration interval is the average of the pressures at the beginning and at the end of the interval. This scheme of using average lifting pressure is particularly necessary in regions where the pressure is rapidly changing. The method does not give the pressure at the beginning of the first integration interval, that is, at the point $n = 0$. It can be shown that, as the first interval approaches zero, the pressure at the lip ($n = 0$) is obtained by letting the expression in equations (23) and (24)

$$\sum_{i=1}^{n-1} \frac{B^2 K_1}{2\alpha V} \left[\sqrt{(T_{i-1}^{n-1})^2 - 1} - \sqrt{(T_i^{n-1})^2 - 1} \right]$$

have the value 0.5 when $n = 1$.

COMPARISON OF THEORY AND EXPERIMENT

Calculations were made to obtain the pressure drag, lift, and moment of the open-nose body on which tests had been made. Figure 1 shows a diagram of the body for which the calculations were made, with the integration stations at which the boundary conditions were applied. The computations were made for the Mach numbers 1.45, 1.60, 1.75, and 3.00.

The experimental drag results had a considerable amount of skin drag and a drag comparison was not therefore conclusive. Estimates of the skin-friction coefficient showed, however, that the calculated drag was of the right order. The agreement of the experimental lift and moment coefficients with the calculated results was quite good. Figure 2 gives a comparison of the lift- and moment-coefficient curves with the experimental data. The effect of the internal flow on the lift can be seen from momentum considerations to be $\Delta C_L = 2\alpha$, whereas the moment which is taken about the midpoint of

the fuselage is $\Delta C_m = a$. These increments have been added to the calculated results for the comparison. In the tests, a tail-surface supporting ferrule was placed over the tail section, and no experimental differences in lift and moment could be detected. It was concluded, therefore, that the thickening of the boundary layer ahead of the shock at the trailing edge was (in effect) forming a ferrule tail when the ferrule was not actually in place. Additional calculations were then made for the shape with the ferrule tail and, as can be seen in figure 2, the agreement with experiment was improved.

The general results of the computations are interesting as they show the effect of Mach number on the body characteristics. In figure 3 the lift-curve slope C_L/a_{deg} shows an increase with increasing Mach number as is the case with projectiles, tests of which were made in Germany and Italy and reported in reference 7. The pressure-drag coefficient C_D drops off, as would be expected. The effect of Mach number on moment and lift can be better illustrated by plotting the effective lifting pressures for different Mach numbers. In figure 4 the distribution of incremental surface pressure coefficients $\Delta p/a_{deg} \cos \theta$ is plotted for $M = 1.6$ and $M = 3.0$. As the Mach number increases, a greater proportion of the lift is shown to be carried over the center section of the body and, as a result, a rearward shift occurs in the center of pressure. Figure 5 shows the distribution of drag pressures over the body. It can be seen that over the conical nose section the pressures fall from the lip-wedge pressures (pressures on a two-dimensional wedge of the same angle, reference 8) to approximately the pressure expected on a cone of the same apex angle (reference 9). At the corners the pressures fall approximately in accordance with the Prandtl-Meyer relation for flow around a corner (reference 9). The method of calculation presented herein is given in more detail in reference 1.

Ferrari (reference 10) has developed the method of characteristics for determining the fields of flow about arbitrary bodies of revolution. His method consists of a step-by-step determination of the pressures and velocities at all points in the field starting from some known boundary. The work involved in obtaining lift and moments is, however, especially tedious as the step-by-step process must be carried out along and around the body.

DIFFUSERS

The problems of obtaining high ram recovery in supersonic flows is of great importance. At high Mach numbers the pressure recovered by a normal shock wave becomes a small fraction of the total pressure in the stream; the total pressure losses through shock waves can be reduced only by a reduction in the Mach number normal to the wave. Interest is therefore centered in the design of diffusers in which the intensity of the shock waves is kept to a minimum. Theoretically a diffuser could be so shaped as to allow smooth isentropic compression through the speed of sound; however, Kantrowitz and Donaldson (reference 2) have shown that such a flow is unstable and unattainable in practice. If, however, a reversed Laval nozzle in which such a flow exists were considered, the Mach number at the minimum-area section would then be unity, corresponding to a maximum mass flow per unit area. Any disturbance in the stream causing a gain in entropy (loss in total head) ahead of the minimum will cause a decrease in the quantity PV_{max} . This decrease in mass flow at the minimum leads to an accumulation of fluid which will immediately cause a normal shock to progress upstream and the mass flow into the diffuser will thus be reduced. If the area of the minimum section is increased, the mass flow can be increased and the shock wave out in front will move down to a position in the diverging passage.

Circular diffusers.- The work of Kantrowitz and Donaldson (reference 2) was done on circular diffusers for the purpose of obtaining designs which, for a specified Mach number, would allow the shock to occur in a region of reduced Mach number, thereby reducing the total-pressure losses through the shock and giving more efficient diffusion. The results of the tests showed that by a suitable choice of contraction ratio (ratio of entrance area to minimum area) the efficiency, even with a long subsonic diffuser, could be made to equal and to exceed, at high Mach numbers, the efficiency obtained by a normal shock alone. Figure 6 shows the test results on three diffusers of different contraction ratios. The efficiency shown in this figure is defined as the ratio of the kinetic energy that the diffused air would have after isentropic expansion to free-stream

pressure to the kinetic energy of the free stream before entering the diffuser. The curves for the diffusers that are designed for the lower Mach numbers fall below the normal shock line. This result, however, is probably the effect of the larger ratio of friction loss to shock loss in the lower supersonic Mach number range. The curve labeled "Crocco's résumé" is one given in reference 11 as the probable efficiency of diffusers for supersonic wind tunnels that have large, well-established boundary layers ahead of the shock.

Annular inlets.— Several proposals have been made for missiles with annular inlets located back on a projectile-shaped nose. Inlets of this type seem to have several outstanding disadvantages. The most serious is the large boundary layer which, in passing through the shock wave in the diffuser, will most certainly cause serious separation. Another problem is that the inlet may be located in a high local Mach number region in which the diffuser efficiency would be again impaired. A preliminary test of such a diffuser has been made in the Langley model supersonic tunnel. As the tests were cut short, only a few points were obtained; however, the best efficiencies found were considerably below those obtained by Kantrowitz and Donaldson. Total-head recovery of the model was 70 percent at a Mach number of 1.55. In the work of Taylor and MacColl (reference 12) on flow over cones, it was found that for large cone angles subsonic flow was produced on the surface of the cone. This result immediately suggests the possibility of an annular diffuser built around a cone. At present, further work is in progress at the Langley Laboratory of the NACA on diffusers of this type. Recent reports of work done in Germany on similar diffusers have indicated that substantial gains in efficiency have been obtained, especially at high Mach numbers.

Variable-area diffusers.— The use of constant-geometry diffusers operating at other than design conditions will probably always result in reduced diffuser efficiencies. If a variable minimum is provided in the diffuser, the local Mach number at which the shock wave occurs can be controlled and kept as close to 1 as stability conditions will permit. It appears that the pressure fluctuations in the combustion chamber of jet-propelled supersonic aircraft will probably limit the shock Mach number to some value slightly above 1 where the shock losses are still insignificant. The exact value of this local Mach number must be determined by

tests of the burners and all components in the ducts behind the shock wave. A movable cone in a fixed cylinder similar to the area-changing device used on several jet-motor exits appears to offer possibilities for use as a variable-geometry diffuser; it is also possible that a rubber area-changing device similar in operation to wing de-icer boots would make a simple easily controlled variable diffuser.

CONCLUDING REMARKS

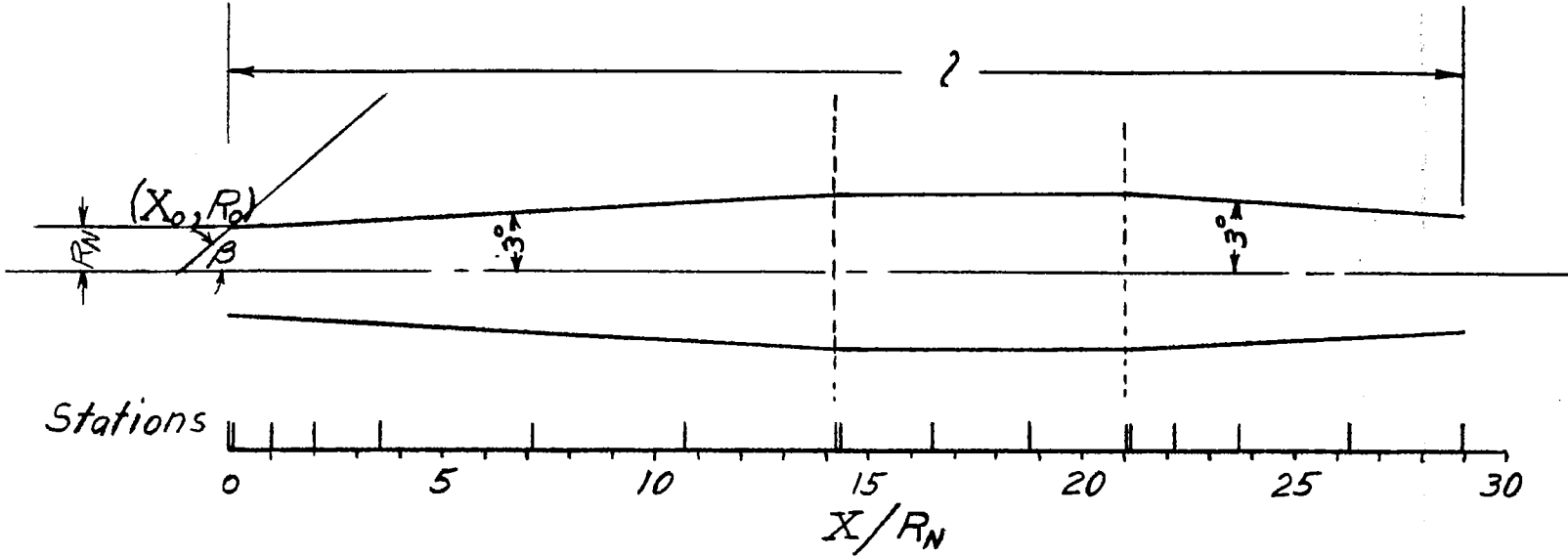
Flight in the supersonic speed range will undoubtedly require airplanes of high aerodynamic refinement. At present, a large and increasing amount of theoretical work is available on this subject. The lift and moment characteristics of ducted bodies at supersonic speeds, obtained by the method presented, were shown to give excellent agreement with available experimental data. A great need is evident, however, for more test data at high Mach numbers, since theory in this field is well in advance of experiment.

Langley Memorial Aeronautical Laboratory
National Advisory Committee for Aeronautics
Langley Field, Va.

REFERENCES

1. Brown, Clinton E., and Parker, Hermon M.: A Method for the Calculation of External Lift, Moment, and Pressure Drag of Slender Open-Nose Bodies of Revolution at Supersonic Speeds. NACA ACR No. L5L29, 1946.
2. Kantrowitz, Arthur, and Donaldson, Coleman duP.: Preliminary Investigation of Supersonic Diffusers. NACA ACR No. L5D20, 1945.
3. von Kármán, Theodor, and Moore, Norton B.: Resistance of Slender Bodies Moving with Supersonic Velocities, with Special Reference to Projectiles. Trans. A.S.M.E., vol. 54, no. 23, Dec. 15, 1932, pp. 303-310.
4. Lamb, Horace: Hydrodynamics. Sixth ed., Cambridge Univ. Press, 1932, p. 527.
5. Ferrari, C.: Campi di corrente ipersonora attorno a solidi di rivoluzione. L'Aerotecnica, vol. XVII, fasc. 6, June 1937, pp. 507-518.
6. Tsien, Hsue-Shen: Supersonic Flow over an Inclined Body of Revolution. Jour. Aero. Sci., vol. 5, no. 12, Oct. 1938, pp. 480-483.
7. Ferri, Antonio: Supersonic-Tunnel Tests of Projectiles in Germany and Italy. NACA ACR No. L5H08, 1945.
8. Ackeret, J.: Air Forces on Airfoils Moving Faster Than Sound. NACA TM No. 317, 1925.
9. Taylor, G. I., and MacColl, J. W.: The Mechanics of Compressible Fluids. Two-Dimensional Flow at Supersonic Speeds. Vol. III of Aerodynamic Theory, div. H, ch. IV, sec. 5, W. F. Durand, ed., Julius Springer (Berlin), 1935, pp. 243-246.
10. Ferrari, C.: Determination of the Pressure Exerted on Solid Bodies of Revolution with Pointed Noses Placed Obliquely in a Stream of Compressible Fluid at Supersonic Velocity. R. T. P. Translation No. 1105, British Ministry of Aircraft Production. (From Atti R. Accad. Sci. Torino, vol. 72, Nov.-Dec. 1936, pp. 140-163.)

11. Crocco, Luigi: Gallerie aerodinamiche per alte velocità. L'Aerotecnica, vol. XV, fasc. 3, March 1935, pp. 237-275 and vol. XV, fasc. 7 and 8, July and Aug. 1935, pp. 735-778.
12. Taylor, G. I., and MacColl, J. W.: The Air Pressure on a Cone Moving at High Speeds. Proc. Roy. Soc. (London), ser. A. vol. 159, no. 838, Feb. 1, 1933, pp. 278-311.



NATIONAL ADVISORY
COMMITTEE FOR AERONAUTICS

Figure 1.- Location of integration stations and intervals on ram-jet body.

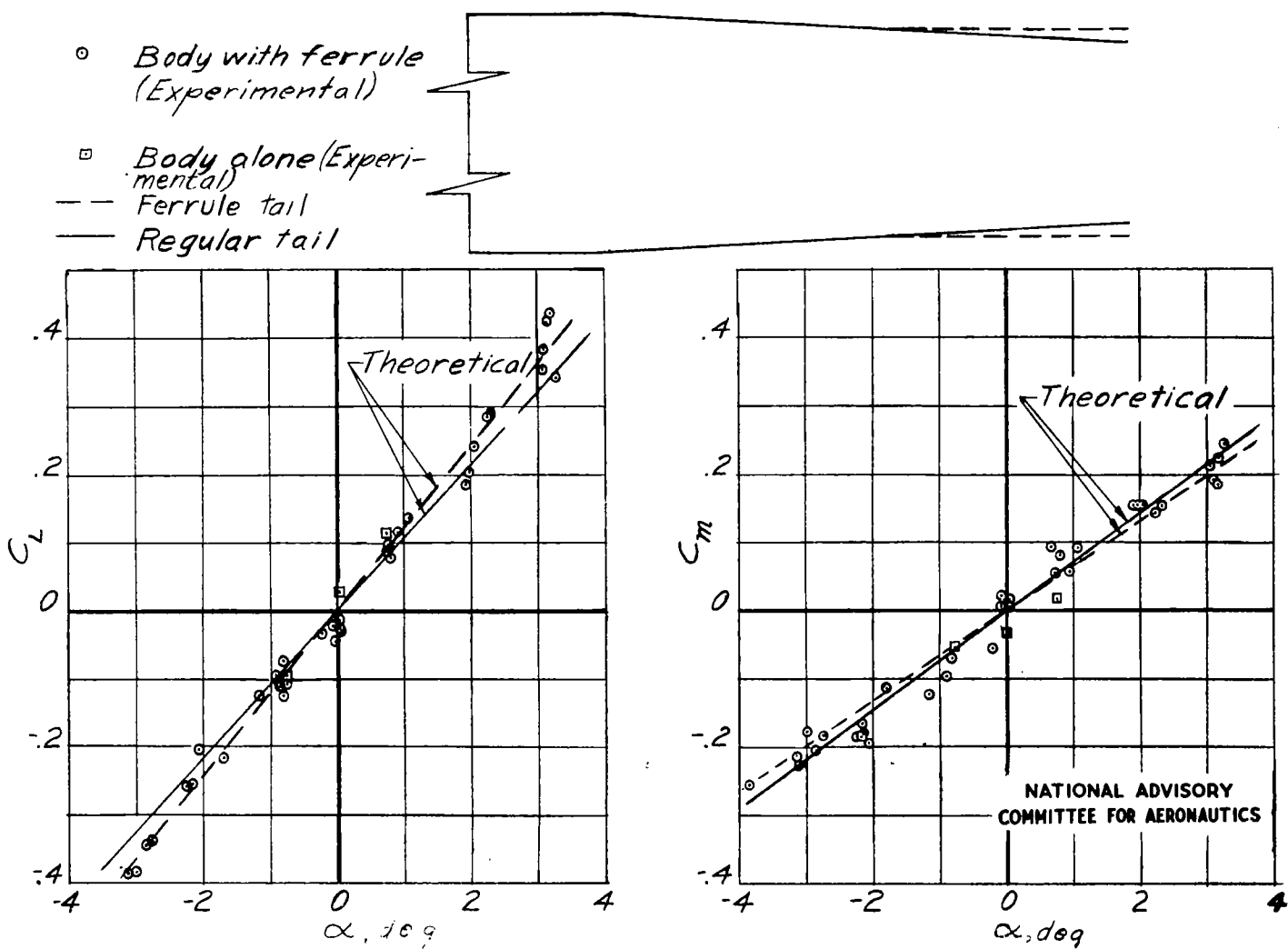


Figure 2.- Comparison of calculated lift and moment coefficients with experimental data.
 $M = 1.45$.

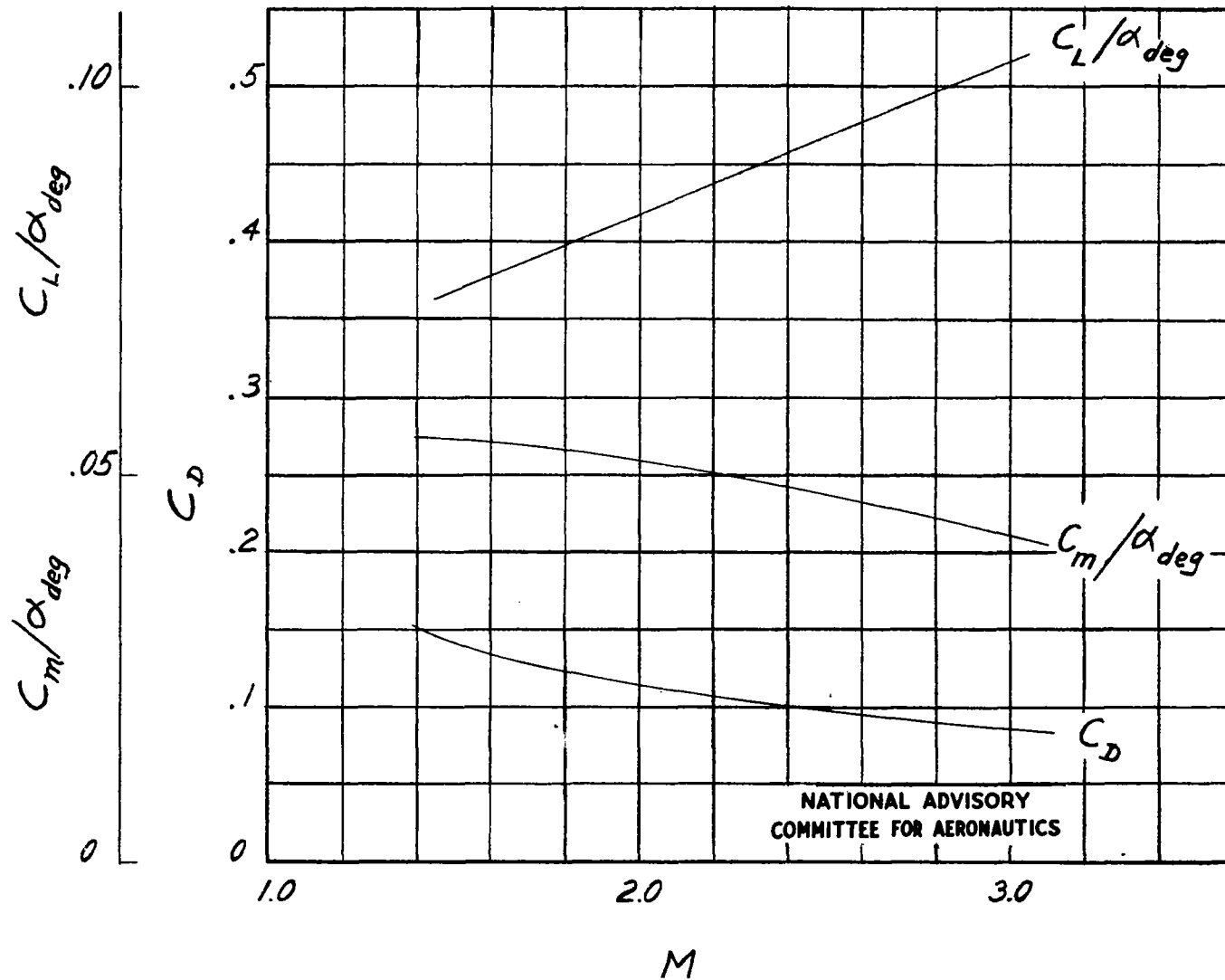


Figure 3.- Theoretical variation of lift, moment, and drag coefficients with Mach number.

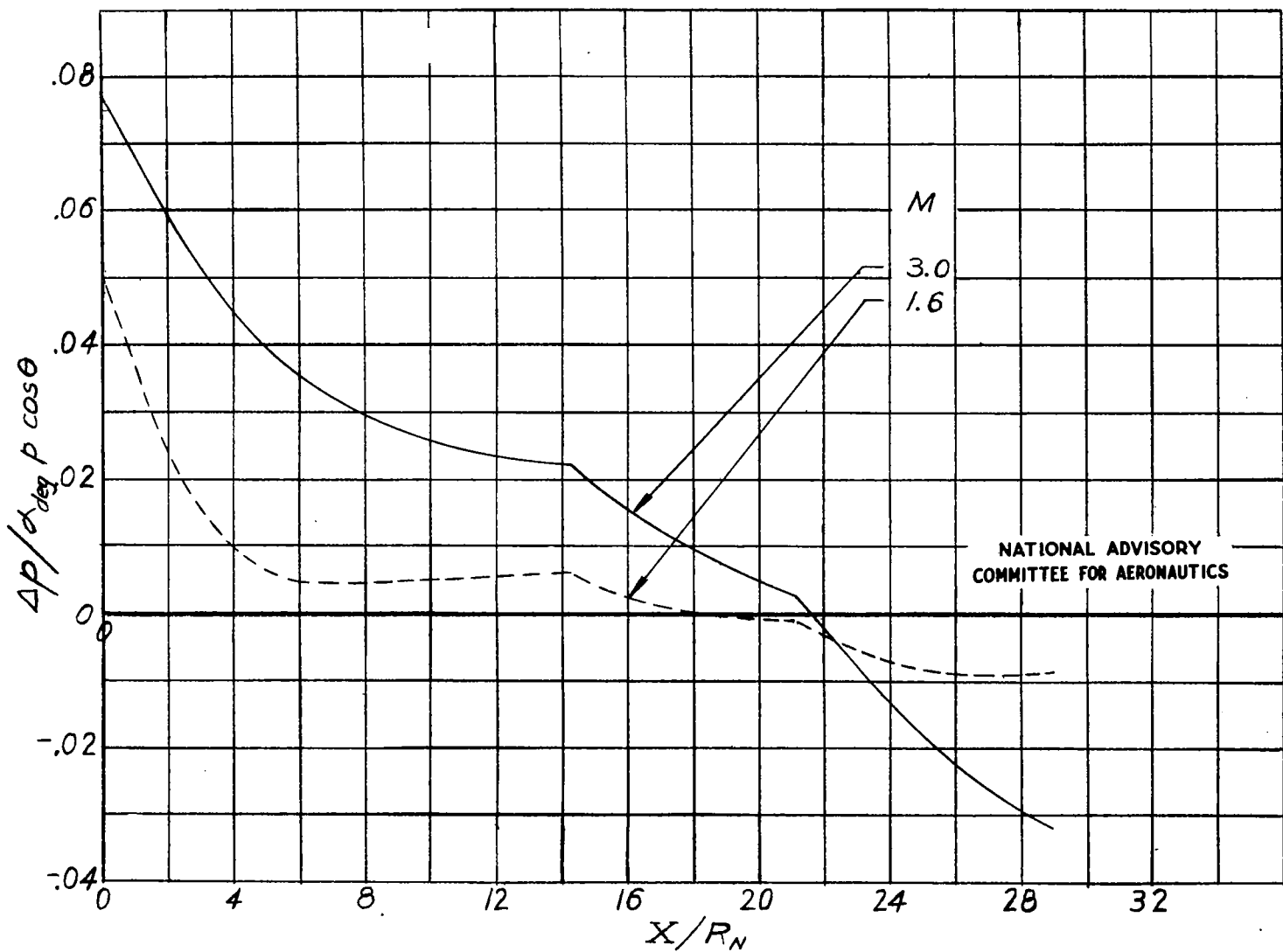


Figure 4.- Distribution of incremental surface pressures over the body at two Mach numbers.

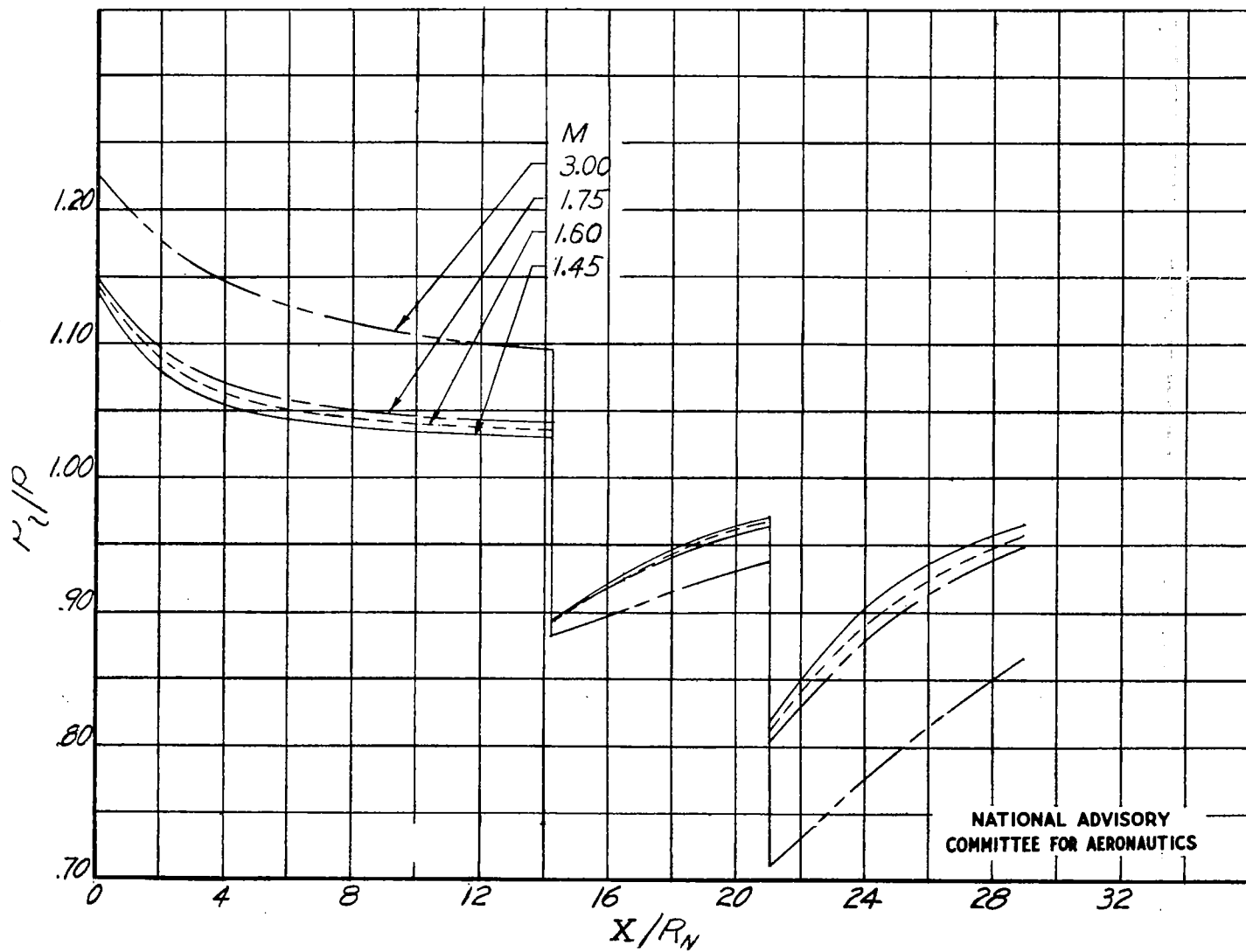
Figure 5.- Calculated pressure distributions for $\alpha = 0^\circ$.

Fig. 6

NACA CB No. L6B26

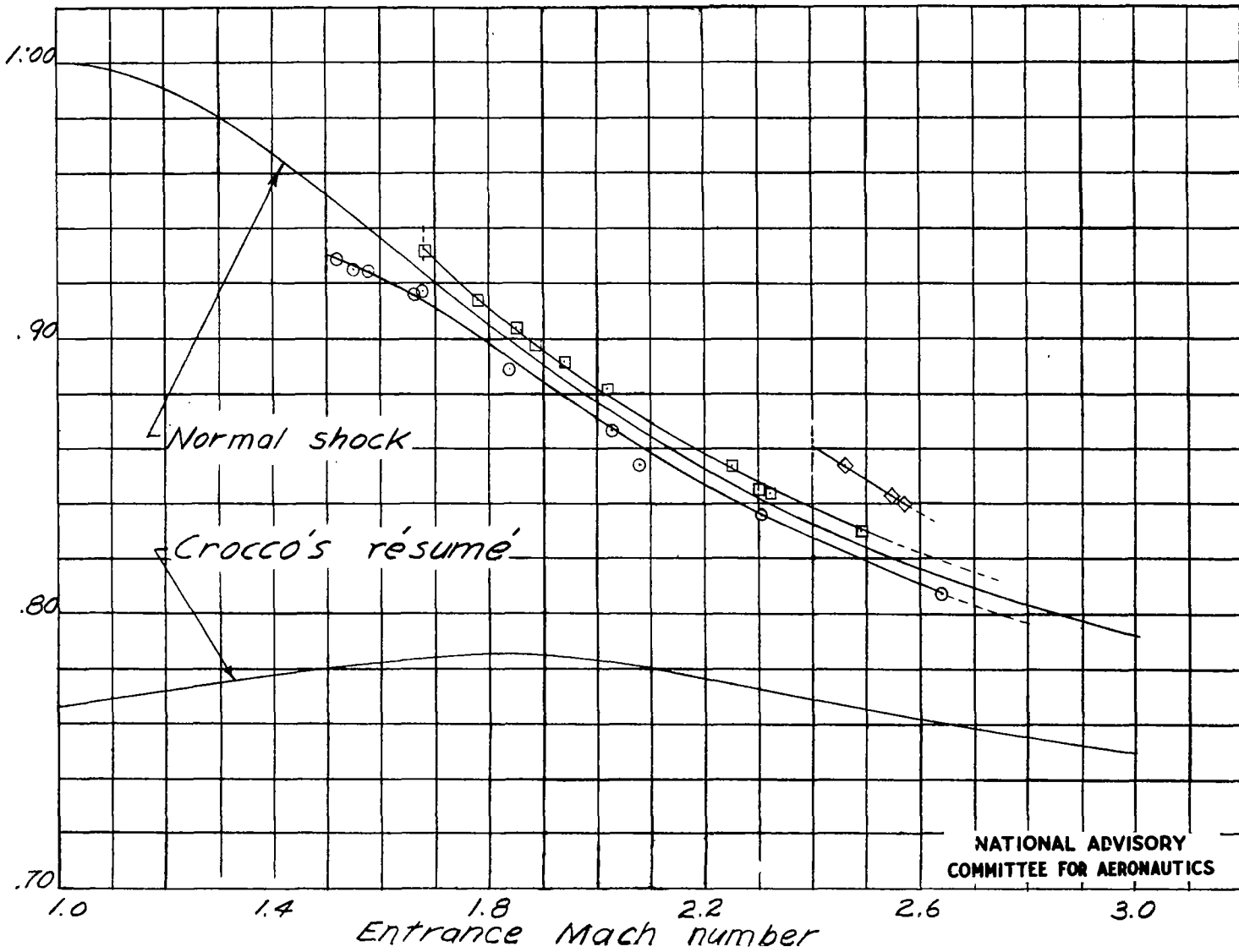


Figure 6.- Diffuser test results of reference 2.

LANGLEY RESEARCH CENTER



3 1176 01348 4887